NASA TECHNICAL TRANSLATION NASA TT F-16981

COMPARISON OF THEORETICAL AND EXPERIMENTAL PROFILE DRAGS

R. Eppler

Translation of "Vergleich theoretischer und experimenteller Profilwiderstände," Schweizer Aero-Revue, Vol.38, No. 10, Oct. 1963, p. 593-595

NATIONAL AERONAUTICS AND SPACE ADMINISTRATION
WASHINGTON, D.C. 20546 APRIL 1976

STANDARD TITLE PAGE

1. Report No.	2. Government Accession No.	3. Recipient's Catalog No
NASA TT F-16981		

4. Title and Subtitle	5. Report Date
COMPARISON OF THEORETICAL AND EXPERIMENTAL PROFILE DRAGS	April 1976
	6. Performing Organization Code

7. Author(s)	8. Performing Organization Report No.
R. Eppler	
	10. Work Unit No.
	11. Contract or Grant No. NASw-2790

9. Performing Organization Name and Address	13. Type of Report and Period Covered
Leo Kanner Associates, Redwood City, California 94063	Translation

12. Sponsoring Agency Name and Address	14. Sponsoring Agency Code
National Aeronautics and Space Administration, Washington D.C. 20546	

15 Supplementary Notes

Translation of "Vergleich theoretischer und experimenteller Profilwiderstände," Schweizer Aero-Revue, Vol. 38, No. 10, Oct. 1963, p. 593-595.

16. Abstract

Experimental drags are compared with calculated values, the latter obtained from potential theory and boundary-layer theory. When there is no separation, agreement is good. The theory also predicts the point at which the "separation level" appears, but not the drag from then on. Small separations are found to be more detrimental to lift than to drag.

17. Key Words (Selected by Author(s))	18. Distribution Statement
	Unclassified-Unlimited

19. Security Classif. (of this report)	20. Security Classif. (of this page)	21. No. of Pages	22. Price
Unclassified	Unclassified		

1. Introduction

Recently, theoretically determined profile drags have been /593* used with increasing frequency in the selection of a profile, for instance for the sailplanes FS 24 Phoenix [1], SB 6 [2], SB 7 and BS 1. Comparing such theoretical drags with experimental results shows the extent to which this procedure is valid, saving, as it does, a considerable amount of time and money.

2. Features of Theoretical Drag Calculation

The calculation of the theoretical drag starts from pressure distributions around the wing profiles, as derived from potential theory. With the aid of boundary-layer theory, the associated friction drags are determined. This means that the so-called form drag of wing profiles, which is based on more extensive flow separation, is not calculated. It is true that boundary-layer theory can provide clues as to the expected point of separation of the flow, and thus establish whether an additional form drag can be anticipated; it says nothing, however, about the magnitude of this drag. Hence, the theoretical drag does not mean much unless friction drag alone is the crucial factor. It will turn out that this is true over a wider range than had been generally believed.

Calculating friction drag requires a certain amount of care, if the results are to be reliable. In particular, the calculation should take into account the difference between laminar and turbulent friction, and thus the transition from a laminar boundary layer to a turbulent one. This is accomplished with the aid of various advances in the field of boundary-layer calculations, which are currently being published [3]. For the boundary-layer transition, one must not only find the instability

---

*Numbers in the margin indicate pagination in the foreign text.

of the laminar boundary layer, but also recognize that there will be a certain distance, depending on the so-called Reynolds number Re, between the instability and the beginning of the turbulent boundary layer, i.e. the transition. Determination of this distance draws on experimental results.

The boundary-layer transition requires particular attention in another respect as well. At low Reynolds numbers, the turbulent boundary layer frequently develops in experiments some distance beyond the end or separation of the laminar boundary layer [4]. Theory also provides clues to this phenomenon, frequently called a "separation bubble." As reported in detail in [3], if the theory does not find the boundary-layer transition to be ahead of the laminar separation point (at low Re numbers), the calculation must be continued from the latter point, starting immediately with the formulas for the completely turbulent boundary layer. Although this does not correctly reflect conditions in a laminar bubble, it has been found that the energy exchange allowed for in the turbulent boundary layer is frequently not sufficient to rapidly eliminate the tendency of the laminar boundary layer to separate. In place of the separation bubble, a turbulent boundary layer is then calculated, the form of which remains close to separation for some distance. This purely theoretical result, termed a "bubble analog" has many parallels with the separation bubble. It almost never occurs unless the laminar calculation proceeds to separation, without the transition condition being satisfied, and it is very sensitive to the pressure distribution near the separation point. If, following laminar separation, there is a stretch with a low pressure gradient, a healthy turbulent boundary layer can develop down to Reynolds numbers about $0.25 \cdot 10^6$; if, in the calculation, laminar separation is followed by a steeper pressure gradient, the bubble analog appears up to $Re \approx 2.5 \cdot 10^6$.

Since, in the bubble analog, there is more energy transport to the wall than should be present in the bubble itself, it seems reasonable to expect bubbles in experiments whenever the theory exhibits a bubble analog; at least one goal in the theoretical development of profiles ought to be the disappearance of the bubble analog.

As in the case of final separation, this analog cannot account for the drag increase generated by the bubble itself. It can only indicate that an additional bubble drag of unknown magnitude must be expected. In all the theoretical drag curves below, this is indicated by showing them as solid lines without the bubble analog, and as broken lines with it. A theoretical drag curve is therefore too favorable by an unknown amount, when it is a broken curve. This will be illustrated by the following diagrams.

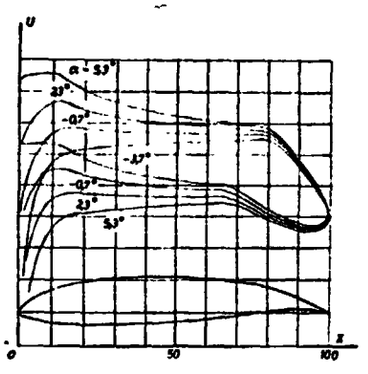

Fig. 1. The theoretically and experimentally studied profile with velocity distributions U (x) for 4 angles of attack.

3. Theoretical Results for an Example

Fig. 1 depicts a wing profile with some potential-theoretical velocity distributions U (x). This is the well-known picture. For a large angle of attack α, the velocity U at the nose is large on the upper side and small on the lower side. Accordingly, if α is large, there is a large velocity drop (pressure gradient) on the upper side, and a small one on the lower side. The angles of attack always are expressed relative to the horizontal line in Fig. 1.

The mathematical method by which the potential-theory connection between profile shape and velocity distribution is determined is not inherently important, as long as the neglected terms are not too large. The methods of conformal mapping [5] /594 and of assuming singularities along the profile contour [6] are nevertheless preferable to approximations which assume singularities along the profile chord. The profile depicted in Fig. 1 was calculated by methods of [5] from certain properties of the velocity distribution, described e.g. by A. Raspet [7]. A change in the angle of attack is easy to handle once the velocity distribution is known for one value of α. In reality, many more values of α were allowed for than are shown in Fig. 1.

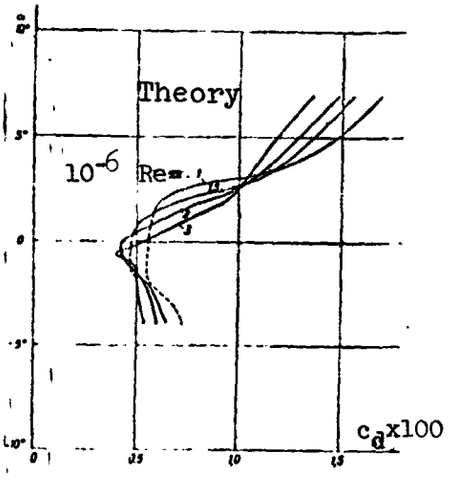

Fig. 2. Theoretical drag coefficients c_a for 4 Reynolds numbers, plotted against α.

For each velocity distribution corresponding to one of the many values of α, the boundary-layer calculation was carried out for four Re numbers. The calculated drag coefficients c_a are plotted against α in Fig. 2. As mentioned in the preceeding section, the bubble analog is indicated by a broken line. Therefore, additional bubble drag must be anticipated where the curves are broken.

4. Comparison with Experimental Drags

The profile of Fig. 1 was studied not only theoretically, but also experimentally in great detail. Fig. 3 depicts the experimental curves corresponding precisely to those in Fig. 2 with respect to Reynolds number and scale. The experimental

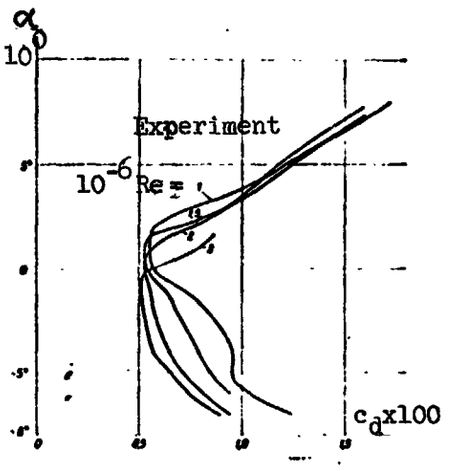

Fig. 3. Experimental drag coefficients c_d for 4 Re numbers, plotted against α.

curves were obtained with a high degree of accuracy by F. X. Wortmann and G. Althaus.[1] At first, the theoretical curves do not seem very similar to the experimental ones. The comparisons of theoretical and experimental curves shown in Figs. 4 through 7 for the four Reynolds numbers demonstrate, however, that the large discrepancies occur almost entirely where the theoretical lines are broken, and thus where the theory suggests the risk of laminar bubbles. In fact, the bubbles were always clearly recognized in the experiments, whenever the drags were unexpectedly large.

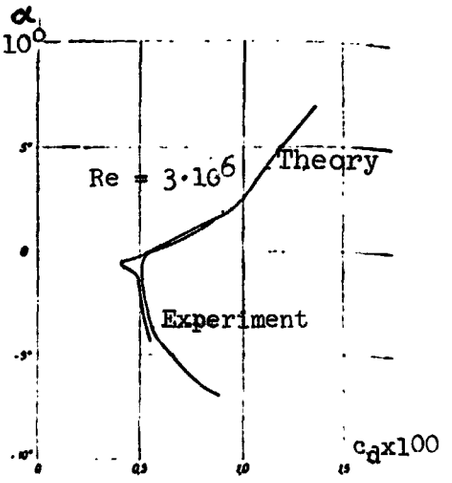

Fig. 4. Comparison of theoretical and experimental curves for c_d (α) at Re = $3 \cdot 10^6$.

Individually, the diagrams provide even more information. Fig. 4 shows that the calculated drag coefficients agree excellently with theory at Re = $3 \cdot 10^6$, and only the very small laminar "bucket" within which theory predicts laminar flow on the upper and lower sides simultaneously, was not confirmed by the experiment. This is not surprising, since the measured points are further apart than the calculated ones, and since the laminar

[1] Institute for Aeordynamics and Gas Dynamics at Stuttgart Technical Academy, Prof. A. Weise.

boundary layers are close to transition, which will make the measurements very sensitive and will tend to scatter them. Note particularly the agreement outside the laminar bucket, where either the upper side or lower side has a predominantly turbulent boundary layer.

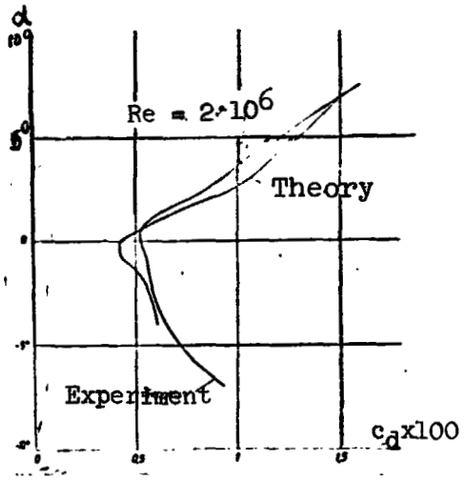

Fig. 5. Comparison of theoretical and experimental curves for c_a (α) at Re = $2 \cdot 10^6$.

Fig. 5 depicts the comparison at Re = $2.0 \cdot 10^6$. Here again, the theoretical bucket is not found in the experiment; otherwise, the agreement is good.

With the Reynolds number of Re = $1.5 \cdot 10^6$ for the diagram in Fig. 6, theory for the first time exhibits a bubble analog, namely for small angles of attack on the upper side of the profile. This immediately makes the agreement much worse, although the theoretical results remain good in the other regions, including the laminar bucket.

For the smallest of the four Reynolds numbers, namely Re = 10^6, there is even more bubble analog in the theory, occurring to some extent on the underside of the profile as well. The experiment (Fig. 7) also exhibits the bubble, and correspondingly high drag. Where there are no bubbles, the theoretical laminar bucket is reproduced well, together with the region above it.

On the whole, theory thus provides good results, particularly with regard to bubble analogs. If theory does not predict this analog for practical flight situations, the risk of an actual

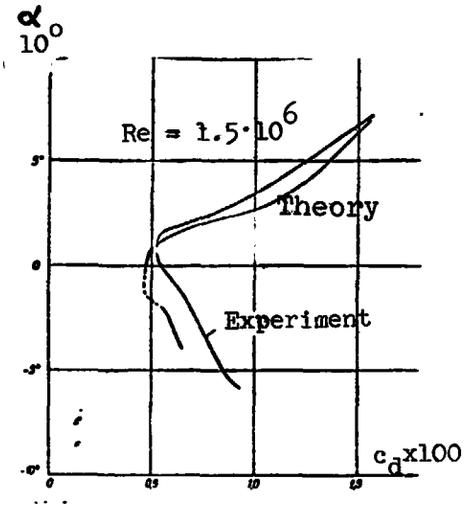

Fig. 6. Comparison of theoretical and experimental curves for $c_a(\alpha)$ at $Re = 1.5 \cdot 10^6$.

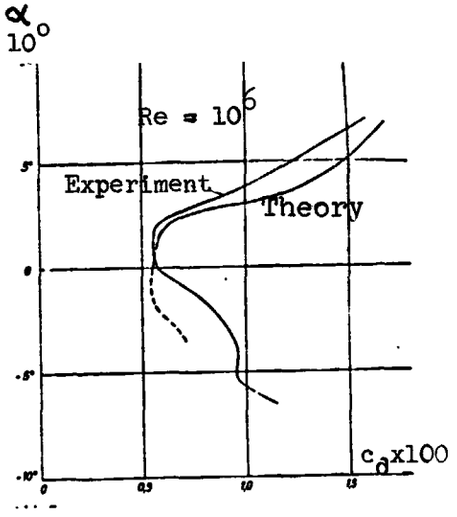

Fig. 7. Comparison of theoretical and experimental curves for $c_a(\alpha)$ at $Re = 1.0 \cdot 10^6$.

occurence of bubbles will also be small. Of course, it must be remembered that in free flight with falling angle of attack, the Reynolds number increases. In our example, this means that few bubbles must be feared in free flight, since the small angles of attack, for which bubbles occur at small Reynolds numbers, will only be achieved at high speeds and thus high Reynolds numbers. Nevertheless, the profile in Fig. 1 is no longer the best calculated one. We used it as an example, because it is the one for which the most exhaustive measurements have been made.

5. Lift Properties

Although the principal purpose of this report is to examine the theoretical drag calculation, a brief comparison with regard to lift would still be valuable, since the dependence of drag on lift is crucial for aircraft performance.

Potential theory yields only the angle of attack of zero lift and increase in the lift

coefficient c_1 for the profile. This is the straight line shown in Fig. 8. It is known that this potential-theoretical lift is not achieved, because of boundary-layer displacement and small flow separations near the trailing edge. Attempts /595
have been made, e.g. in [8], to estimate the effect of boundary-layer displacement on lift. This would also be easy to do with the present boundary-layer results. However, in many cases, the primary effect will be that of small boundary-layer separations near the trailing edge. Theoretical analysis of this effect is a field in itself, and involves problems which probably cannot be solved reliably except by wake theory. However, the general case in that theory has not been solved mathematically.

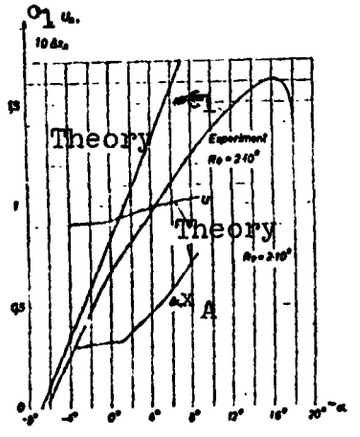

Fig. 8. Theoretical and experimental curve for lift coefficient c_1 as a function of α. Position of point of separation on the upper side and velocity at this point.

Since boundary-layer theory provides at least a clue to the point of separation, experimental lift loss can be compared with the position of the point of separation at Re = $2 \cdot 10^6$ in Fig. 8. Δx_A denotes the distance from the point of separtion on the upper side to the trailing edge (relative to profile chord). For simplicity, the scale for plotting this variable in Fig. 8 is the same as the c_1 scale. It should therefore be noted that for 10 Δx_A = 0.5, separation occurs 0.05 chord depths or 5% of the chord length from the trailing depth. The separations shown are therefore always small. Nevertheless, there is a conspicuous relationship between Δx_A and lift loss. Even at α = 0, where the separation begins

to migrate forward at a very slow rate, and appreciable lift loss can be observed. It is noteworthy that the separations do not cause any major increase in drag in the angle-of-attack region of this lift loss, as indicated by Fig. 5. This is consistent with the results of wake theory, according to which flow separation does not cause drag to increase as long as the flow velocity at separation is no greater than the relative air speed [9]. Therefore, Fig. 8 also includes the ratio U between flow velocity at the calculated point of separation and relative air speed. In fact, in the region of interest, this value is not much greater than 1, which confirms the applicability of the wake-theoretical results.

Unfortunately, this finding does not mean that small separations can be tolerated without disadvantage. In many cases, there may well be no increase in drag; nevertheless, the lift loss is just as harmful for the polar diagram, in which drag is plotted against lift. The discovery that the principal harm of small separations is their effect on lift has stimulated further investigations, which will certainly provide a number of valuable results.

6. Summary

Careful comparisons of theoretical and experimental profile drags indicate that the increasing use of theoretical drag calculations is justified.

REFERENCES

1. Nägele, H. and R. Eppler, "Plastic Sailplane FS 24 Phoenix," Schweizer Aero-Revue 33, pp. 140-143 (1958).

2. "Akaflieg Braunschweig is Building a New Sailplane," Deutscher Aero-Club 1962, pp. 1178-1181.

3. Eppler, R., "Practical Calculation of Laminar and Turbulent Section Boundary Layer," Bölkow-Entwicklungen KG, Report FM 134, to appear in Ing.-Arch.

4. Wortmann, F. X., "Experimental Studies on New Laminar Profiles for SailPlanes and Helicoptors," Zeitschr. f. Flugwiss 5, pp. 228-253 (1957).

5. Eppler, R., "Direct Calculation of Airfoil Profiles from the Pressure Distribution," Ing.-Arch 25, pp. 32-57 (1957).

6. Eppler, R., "Calculation of Pressure Distribution on Lattice Profiles in Two-dimensional Potential Flow with a Fredholm Integral Equation," Arch. Rat. Mech. Anal. 3, pp. 235-270 (1959).

7. Raspet, A. and D. Györgyfalvy, "The Phoenix -- One Solution for an Optimum Overland Sailplane," Zeitschr. f. Flugwiss 8, pp. 260-266 (1960).

8. Kraemer, L., "Boundary Layer Calculations for 12 Profiles," AVA Report 55 B15, Göttingen 1955.

9. Eppler, R., "Contributions to Theory and Application of Discontinuous Flows," J. Rat. Mech. Anal. 3, pp. 591-644 (1954).